Loss-of-function mutations in the melanocortin-1-receptor (Mc1r) cause disruption of dorso-ventral countershading in teleost fish

Laura Cal[1], Paula Suarez-Bregua[1] , Ingo Braasch[2], Uwe Irion[3], Robert Kelsh[4], Jose Miguel Cerdá-Reverter[5*&,] Josep Rotllant[1*&.]

Short title: Fish pigmentation and melanocortin system

[1] FishBioTech Lab. Department of Biotechnology & Aquaculture. Institute of Marine Research, (IIM-CSIC), 36208 Vigo, Spain.

[2]Department of Integrative Biology and Program in Ecology, Evolutionary Biology and Behavior, Michigan State University, East Lansing, MI 48824, USA.

[3]Max-Planck-Institut of Developmental Biology, Tübingen, Germany

[4]Department of Biology and Biochemistry and Centre for Regenerative Medicine, University of Bath, Claverton Down, Bath, BA2 7AY, United Kingdom.

[5]Department of Fish Physiology and Biotechnology, Institute of Aquaculture from Torre la Sal (IATS-CSIC), Castellon, Spain. 12595, Spain.

[*]Corresponding authors and reprint requests:

Josep Rotllant, Instituto de Investigaciones Marinas, CSIC. Eduardo Cabello, 36208, Vigo (Pontevedra), Spain

Tel. (+34) 986-231930 Fax (+34) 986 292 762

E-mail: rotllant@iim.csic.es

25 Jose Miguel Cerdá-Reverter, Instituto de Acuicultura de Torre de la Sal, CSIC. Torre
26 la Sal s/n, 12595, Ribera de Cabanes, Castellón, Spain
27 Tel. (+34) 964319500 Fax (+34) 964319509
28 E-mail: jm.cerda.reverter@csic.es
29
30 [&]Co-senior authors

ABSTRACT

The Melanocortin 1 receptor (MC1R) is the central melanocortin receptor involved in vertebrate pigmentation. Mutations in this gene cause variations in coat coloration in amniotes. Additionally, in mammals MC1R is the main receptor for agouti signaling protein (ASIP), making it the critical receptor for the establishment of dorsal-ventral countershading. In fish, Mc1r is also involved in pigmentation but it has been almost exclusively studied in relation to melanosome dispersion activity and as a putative genetic factor involved in dark/light adaptation. However, its role as the crucial component for the Asip1-dependent control of dorsal-ventral pigmentation remains unexplored. Using CRISPR/Cas9 we created *mc1r* homozygous knockout zebrafish and found that loss-of-function of mc1r causes a reduction of countershading and a general paling of the animals. We find ectopic development of melanophores and xanthophores, accompanied by a decrease in iridophore numbers in the ventral region of *mc1r* mutants. We also reveal subtle differences in the role of mc1r in repressing pigment cell development between the skin and scale niches in ventral regions

Keywords: Mc1r, Asip1, pigmentation, melanophores, xanthophores, iridophores, chromatophore, zebrafish, countershading, CRISPR

SIGNIFICANCE

Countershading is a widespread pigmentary adaptation throughout vertebrates and graded agouti-signaling peptide (ASIP) is the main regulatory effector. In mammals, *Asip* expression signals through melanocortin receptor type-1 (MC1R) to inhibit melanogenesis and melanocyte differentiation *in vitro*. Strikingly, in fish Asip-dependent dorso-ventral patterning depends upon multiple types of chromatophore,

but the skin expresses multiple MCRs and the role for Mc1r remains untested. We show here that Mc1r is required to block melanophore and xanthophore, and to promote iridophore, development in ventral skin. In contrast, loss of Mc1r function only partially reduced melanophores and xanthophores dorsally, suggesting involvement of additional signaling systems.

INTRODUCTION

Pigment patterns have always intrigued scientists for both their evolutionary and developmental aspects, and fish constitute excellent models because of their great color pattern diversity. Zebrafish (*Danio rerio*) has become an important model to study color pattern formation and cell fate decisions in vertebrates. Its striped pigmentation is achieved by the patterned distribution of three types of pigment cells (chromatophores), melanophores, xanthophores and iridophores. Both melanophores and xanthophores absorb light due to the synthesis of melanin and pteridine pigments, respectively; whereas iridophores reflect light because of guanine crystals (Hirata et al., 2003, Hirata et al., 2005) . This striped pattern is superimposed on an ancient dorso-ventral countershading pattern, with dark dorsum and light ventrum (Cal et al., 2017; Ceinos et al., 2015). Dorso-ventral pigment polarity is a highly conserved evolutionary trait (Linnen et al., 2013). It is regulated by the local presence/absence of agouti-signaling protein (ASIP, simply called Agouti in mouse) (Vrieling et al., 1994). In mammals ASIP binds to the melanocortin receptor 1 (MC1R), encoded by the extension (e) locus, and which is the receptor for melanin-stimulating hormone (MSH) (Robbins et al., 1993). Binding of agouti to MC1R lowers the ratio of eumelanin (dark/brown pigment) to pheomelanin (red/yellow pigment) produced in the melanocytes (mammalian melanophores) (Michaud et al., 1993; Miller et al., 1993),

inhibits melanoblast differentiation and proliferation (Aberdam et al., 1998; Sviderskaya et al., 2001) and promotes dedifferentiation of melanocytes *in vitro* (Le Pape et al., 2009). Agouti expression in different regions of the body is controlled by distinct regulatory regions of the agouti gene. It results in either ventral specific or hair cycle specific isoforms controlled by distinct regulatory enhancer regions of the *agouti* gene. These result in either ventral specific or hair cycle specific isoforms. The ventral isoform is constitutively expressed during development thus driving melanocytes to synthesize pheomelanin and resulting in pale coloration. Dorsal-specific isoform expression is temporally regulated during the hair cycle, thus producing the distinctive yellow subapical band of the agouti fur coloration (Vrieling etal., 1994). Dorsoventral pigmentation gradients in fish also depend on a dorso-ventral expression gradient of Asip1 (the fish ortholog of mammalian ASIP) (Cerdá-Reverter et al., 2005; Ceinos et al., 2015; Guillot et al., 2012;), but the cellular and biochemical mechanisms seem to be different from that of mammalian species. Fish melanophores synthesize only eumelanin (Kottler at al., 2015), therefore changes in dorsoventral pigmentation can be achieved either by inhibition of melanogenesis or by differential chromatophore distribution. In zebrafish, *asip1* overexpression inhibits melanogenesis in the dorsal region (Ceinos et al., 2015; Guillot et al., 2012) by antagonizing melanocortin signaling (Cerdá-Reverter., 2005), but it also promotes the proliferation of dorsal iridophores (Ceinos et al., 2015). Accordingly, asip1 knockout has no effect on dorsal pigmentation but the lack of Asip1 in the belly promotes a dorsalization of the ventral pigmentation by increasing melanophore differentiation and xanthophore numbers in parallel with the disappearance of most ventral iridophores (Cal et al., 2019). Taken together, the gradient of *asip1* expression is responsible for the dorso-ventral

pigmentation gradient in fish by using a different mechanism from tetrapods, i.e. by inhibiting ventral melanogenesis and modulating chromatoblast fate.

This analysis leaves an important question concerning the signaling mechanism that Asip1 uses in zebrafish to regulate pigmentation. To date, five different melanocortin receptors (Mc1r-Mc5r) have been characterized in vertebrates (Cortés et al., 2014). Mc2r is unique because it is exclusively activated by the adrenocorticotropic hormone (ACTH) and it requires the interaction with the melanocortin receptor accessory protein 1 (Mrap1) (Cerdá-Reverter et al., 2013). All other receptors bind the diverse MSH-ligands with different affinities (Schiöth et al.,. 2005), and ACTH can also activate Mc4r in combination with Mrap2 (Agulleiro et al., 2013). Asip1 has been shown to antagonize the effects of Msh on Mc1r and Mc4r in goldfish (Cerdá-Reverter et al., 2005). In addition, Asip1 can inhibit (Nle4, D-Phe7)-α-MSH-stimulated melanosome dispersion (Cerdá-Reverter et al., 2005). Zebrafish has six melanocortin receptors, since Mc5r is duplicated, as Mc5ra and Mc5rb (Cortés etal., 2014). They are antagonized by Asip1 but the protein seems to work also as an inverse agonist at Mc1r (Guillot et al., 2012), with low Mc1R activity occurring in the absence of MSH or the presence of Asip1. Although the involvement of Mc1r signaling in the agouti phenotype of zebrafish has been suggested, we cannot rule out the participation of other Mcr receptors since their expression in fish skin has been reported, e.g. Mc4r in cyprinids (Cerdá-Reverter et al., 2003; Wei et al., 2013), Mc5r in flatfishes, goldfish, and bass (Cerdá-Reverter et al., 2003; Kobayashi et al., 2012; Sánchez et al., 2009) and Mc2r in bass (Agulleiro et al., 2013). Here, we investigate the role of Mc1r in zebrafish pigmentation *in vivo* by generating knockout mutants using the CRISPR/Cas9 genome-editing tool (Bassett et al., 2013). We demonstrate a disruption of the dorso-ventral pigmentation polarity in *mc1r* knock-out fish, consistent with it

being the key receptor mediating Asip1 function in zebrafish dorsoventral countershading.

MATERIALS AND METHODS

Fish

Zebrafish were cultured as previously described (Westerfield., 2007) and staged by standard criteria (Kimmel et al., 1995). Fish of the following genotypes were used: TÜ strain (Tübingen, Nüsslein-Volhard Lab), Tg(Xla.Eef1a1:Cau.Asip1)iim05 (Ceinos et al., 2015), Tg(TDL358:GFP)(Levesque et al., 2013) , Tg(kita:GalTA4:UAS:mCherry) (Anelli et al., 2009). Ethical approval (Ref. Number: AGL2011-23581) for all studies was obtained from the Institutional Animal Care and Use Committee of the IIM-CSIC Institute in accordance with the National Advisory Committee for Laboratory Animal Research Guidelines licensed by the Spanish Authority (RD53/2013) and conformed to European animal directive (2010/63/UE) for the protection of experimental animals.

Generation and analysis of mc1r knockout mutants

The *mc1r* loss-of-function mutation was generated using the CRISPR-Cas9 gene editing system. The CRISPR protocol, originally adapted from Bassett et al. (Bassett et al., 2013), was kindly provided by Sam Peterson (U Oregon). The possible target sequence was identified with the ChopChop web tool (Montague et al., 2014). Two long oligonucleotides (Scaffold oligo: 5`-GATCCGCACCGACTCGGTGCCACTTTTTCAAGTTGATAACGGACTAGCCTTATTTTAACTTGCTATTTCTAGCTCTAAAAC-3`, and two different gene-specific oligo GS1: 5'-AATTAATACGACTCACTATAGCTAGTGAGCGTCAGTAATGGTTTTAGAGC

TAGAAATAGC-3' and GS2: 5'-AATTAATACGACTCACTATAGGGCCAAGATGAACATGTGCAGGGTTTTAGAGCTAGAAATAGC-3') were used to perform a template-free PCR to obtain a 125 bp DNA fragment that includes the two previously identified target site sequences (TS1: 5'- GCTAGTGAGCGTCAGTAATGTGG-3' and TS2: 5'-GGGCCAAGATGAACATGTGCAGG-3'). The PCR reaction was performed in 20 µL containing 10 µL of 2x Phusion High-Fidelity PCR Master Mix Buffer (New England Biolabs, UK), 1 µL of gene specific oligo (10 µM), 1 µL of gRNA scaffold oligo (10 µM) and H_2O nuclease free to 20 µL. PCR conditions were 98ºC for 30 sec, 40 cycles of 98ºC for 10 sec, 60ºC for 10 sec, 72ºC for 15 sec, and a final step of 72ºC for 10 min. The PCR product was purified using DNA Clean&Concentration-5 Kit (Zymo Research, USA) according to the manufacturer's instructions. Purified PCR product was used as template for in vitro transcription with MEGAscript T7 High yield transcription Kit (Ambion, USA) according to the manufacturer's instructions. The gRNA was purified with RNA Clean&Concentrator 5 (Zymo Research, USA). The gRNA was injected in a concentration of 25 ng/µL together with Cas9 mRNA (from the pT3TS-nCas9n plasmid, Addgene, USA) at 50 ng/µL and Phenol red solution (0,1%). Around 2 nL of this mix was microinjected into zebrafish eggs. Different mutations were found and three different potential non-functional mutations were raised as separate mutant allele lines (see results section). Primer sequence for genotyping PCR were: TS1-F: CTTCAGCATGAAACACATGGA; TS1-R: ATGGTGCACAGAAACGACAA; TS2-F: CTTCAGCATGAAACACATGGA; TS2-R: AAGGGTTTGTGGGACAGGTG. For microscope imaging, zebrafish of 5dpf, 15 dpf, 30 dpf and 210 dpf were anesthetized with tricaine methasulfonate (MS-222-, Sigma-Aldrich), skin sections and scales were isolated from the ventral and

dorsal areas and immersed in PBS on a glass slide and photographed. Transgenic/mutant lines were obtained by setting up crosses between the *mc1r* mutant lines and the reporter transgenic line Tg(TDL358:GFP), which labels iridophores (Levesque et al., 2013), or Tg(kita:GalTA4:UAS:mCherry), which labels melanophores (Anelli et al., 2009). The offspring of these crosses were incrossed to obtain homozygous *mc1r* mutants. Confocal imaging was carried out on a Leica TCS SP5 confocal microscope.

Melanophore and xanthophore counts

The melanophore pattern of *mc1r* knockout mutant fish ($mc1r^{K.O.}$) was compared with control fish by quantification of melanized melanophores in both groups (Fig. 3, 4). Selected regions for melanophore counting were different in each stage of development. In early stage (5dpf), we counted melanophores in a 1 mm^2 area in a dorsal view on the head and the dorsal area, on the horizontal myoseptum and in a ventral view of the head. In early metamorphic stage (15dpf), we counted melanophores in a 1 mm^2 area in a dorsal view on the head, on the dorsal area, on the horizontal myoseptum and in a ventral view of the head and the belly. In late metamorphic stage (30dpf), we counted melanophores in a 1 mm^2 area in a dorsal view on the head, dorsal area, horizontal myoseptum and in a ventral view on the head and belly. In adult fish (60 and 210 dpf) melanophores within 1 mm^2 area were counted in several distinct positions: in a dorsal view on the head (head area) and on the dorsal area (from the edge of the head to edge of the dorsal fin); in a lateral view, on the dorsalmost dark stripe (2D), 1D, first ventral dark stripe under the myoseptum (1V) and 2V anterior areas (pectoral to pelvic fin); and finally, in a ventral view of the head and the belly (pectoral to pelvic fin) (see Fig. 4A; Fig 7Q-T). The dorsal-ventral

xanthophore pattern of *mc1r* knockout fish mutant was compared with control fish by quantification of pigmented xanthophores in post-metamorphic fish (60 and 210 dpf). For xanthophore counting, selected regions on the dorsal area (from the edge of the head to edge of the dorsal fin), and in a ventral view of the belly (pectoral to pelvic fin) were selected (see Fig. 4A). To analyze the number of melanophores and xanthophores, seven fish per group were anesthetized with tricaine methasulfonate (MS-222-, Sigma-Aldrich) and immersed in 10 mg/ml epinephrine (Sigma) solution for 30 min to contract melanosomes. Fish were photographed on a Leica M165FC stereomicroscope equipped with a Leica DFC310FX camera. Melanophores were counted using ADOBE PHOTOSHOP CS2 software (Adobe Systems Software Adobe Systems Ibérica SL, Barcelona, Spain) and the ImageJ software (National Institutes of Health, NIH, Maryland, USA). Data values were statistically evaluated by Student's t-test and data expressed as mean standard error of the mean (SEM).

Functional Asip1/Mc1r interaction

Transgenic/knockout line (*mc1r*$^{K.O.}$*/Asip1-Tg)* were obtained by setting up crosses between the CRISPR1-*mc1r*.iim02 mutant line and the transgenic reporter line Tg(Xla.Eef1a1:Cau.Asip1)iim05 (Ceinos et al., 2015), which ectopically overexpresses *asip1* and produces a dorsal-ventral disruption of pigment pattern phenotype with dorsal skin as pale colored as ventral skin. The offspring was then incrossed to obtain the F2 generation and the *mc1r* locus was sequenced to confirm the homozygous knockout mutation (*mc1r*$^{K.O.}$) that carries the dominant *asip1* transgene, localized by PCR using specific primers for the Tol2 vector (forward: 5'-GCCCCTCTGCTAACCATGTTC-3', reverse: 5'-TCATCAATGTATCTTATCATGTCTGG-3'). Adult double transgenic/mutant

zebrafish (100dpf) were anesthetized with MS-222 and photographed. Microscope imaging was carried out in a Leica M165FC stereomicroscope equipped with a Leica DFC310FX camera.

RESULTS

Generation and selection of induced mc1r loss-of-function mutations

Loss-of-function mutations in the zebrafish *mc1r* gene were generated using the CRISPR/Cas9 system. We selected two different target sites in the single coding exon (target T1: 286 bp after ATG and target T2: 636 bp after ATG) (Fig. 1A, B) and found six different mutated alleles (Fig. 1B). Alleles M1 and M6 conserved the original open reading frame; therefore, they could potentially generate a functional protein lacking only one or two amino acids but keeping most of the complete amino acid sequence. Alleles M2, M3, M4 and M5 show different open reading frames downstream of the target site. The *mc1r* gene encodes a predicted protein of 323 amino acids. We selected three mutations with predicted non-functional protein and established stable homozygous mutant lines of each one to characterize the phenotype: M2 (CRISPR1-*mc1r*.iim02), M3 (CRISPR1-*mc1r*.iim03), and M4 (CRISPR1-*mc1r*.iim04) (Fig. 1B). The $mc1r^{iim02}$ allele lacks 7 bp (Del 264-271) and carries 11 bp insertion at position 264 downstream of the predicted ATG. The $mc1r^{iim03}$ allele has lost 2 bp (Del 642-644), and $mc1r^{iim04}$ lacks 2 bp (Del 642-644) and carries 16 bp insertion at position 642 downstream of the predicted ATG (Fig. 1B). In those three alleles, the mutations result in premature stop codons. The $mc1r^{iim02}$ encodes a 123 amino acids mutant protein with 95 shared amino acids with WT Mc1r , the $mc1r^{iim03}$ encodes a mutant protein with 231 amino acids with 214 shared amino acids with WT Mc1r , and $mc1r^{iim04}$ encodes a mutant protein with 243 amino acids with 214 shared amino acids

with WT Mc1r (Fig. 1C). None of the predicted mutated proteins have the last three α-helical transmembrane (TM) domains and an intracellular C-terminus with a palmitoylation site which are required for ligand-receptor binding and the appropriate tertiary structure of the receptor, therefore none of these mutant proteins would be predicted to retain partial function. All mc1r knockout mutant lines examined resulted in a similar dorso-ventral pigment phenotype as described below.

_mc1r_ functions in dorso-ventral pigment patterning

All three homozygous *mc1r*-CRISPR knockout lines exhibited an indistinguishable reduction of dorso-ventral countershading (Fig. 2), therefore we focused on the study of one homozygous line, CRISPR1-*mc1r*.iim02 (referred to as $mc1r^{K.O.}$). $mc1r^{K.O.}$ fish displayed enhanced pigmentation over the entire ventral region (Fig. 2 B, D, F, H), as well as a significant reduction over the dorsal and lateral regions (Fig. 2 D, J) compared to WT siblings. In particular, in $mc1r^{K.O.}$ fish, the number of melanophores and xanthophores is increased in all ventral regions (Fig 2. G, H) together with a concomitant reduction of these two pigment cell types in all dorsal regions (Fig.2 I, J). This phenotype results in an apparent paling of the animal with a corresponding reduction of countershading. Mutations of the *mc1r* gene had no major effect on the characteristic striped pattern (Fig.2 A-D). However, we observe a significant decrease of melanophore numbers in the dorsal 2D dark stripe, and the incipient 3V-stripe is more pronounced in $mc1r^{K.O.}$ mutants compared to wild type (Fig. 2C,D). In addition, the abdominal ventral region exhibits a decrease in the number of iridophores that results in an apparent breakup of the ventral iridophore layer into smaller fragments, thus conferring a darker color to the ventral region of $mc1r^{K.O.}$ fish (Fig. 2H).

The development of the zebrafish *mc1r*$^{K.O.}$ phenotype

To establish the time point when the phenotype of the *mc1r*$^{K.O.}$ mutants first becomes apparent during development, melanophores were counted at larval (5dpf, SL 3 mm), metamorphic (15 dpf, SL 6.3 mm and 30 dpf, SL 7 mm) and two adult stages (60 dpf, SL 13 mm and 210 dpf, SL 25 mm) (Fig. 3 and 4). It has been shown that pigment pattern changes during development can be quantified by an increase in melanophore numbers and variations in their distribution (Kelsh., 2004; Parichy et al., 2009) . We determined the melanophore distribution in *mc1r*$^{K.O}$ and WT siblings along the dorso-ventral axis, by counting at defined positions in the dorsal and ventral head, the lateral stripes and the belly (see Materials and Methods and Figs. 3 and 4 for details). We found a significant general reduction of melanophore density in *mc1r*$^{K.O.}$ at all developmental stages evaluated. At pre-metamorphic (15dpf) and metamorphic stages, the melanophore density were significantly lower in all areas examined. During pre-metamorphic stages (15dpf), melanophore density was lower in the dorsal, lateral and belly regions of *mc1r*$^{K.O.}$ mutants compared to WT fish (Fig. 3A). During late metamorphosis (30dpf), melanophore density was also lower in the dorsal, lateral region and belly of *mc1r*$^{K.O.}$ mutants compared to WT fish (Fig. 3B). At adult stages (60 and 210 dpf), *mc1r*$^{K.O.}$ mutants exhibited an obvious dorso-ventral pigmentation defect characterized by an increase of melanophore and xanthophore density in the ventral areas (Fig. 4B) together with a significant decrease of melanophore and xanthophore density in the dorsal and lateral body sections, resulting in a general homogenization of melanophores densities across the dorsoventral axis (Fig. 4C). At 60 dpf, the density of melanophores in *mc1r*$^{K.O.}$ mutants compared to WT fish was lower in the dorsal region, the dark stripe 2D, the dark stripe 1D and in the dark stripe 1V. However, in the ventral region of the head, the density of melanophores was higher

in *mc1r*$^{K.O.}$ mutants compared to WT fish. No differences were found in the dark stripe 2V and the belly (Fig. 4C). Additionally, the density of xanthophores was also affected. *mc1r*$^{K.O.}$ mutants show a significant increase in the number of ventral xanthophores ($P<0.01$) compared to WT fish (Fig. 4D). A similar phenotype was found at 210 dpf; melanophore densities in 210 dpf *mc1r*$^{K.O.}$ mutants were considerably lower in the dorsal region of the head, in the dorsal region, in the dark stripe 2D and in the dark stripe 1D compared to WT. In contrast, the density of melanophores in the ventral region, in the dark stripe 3V and in the belly of *mc1r*$^{K.O.}$ fish was significantly higher than in their WT siblings (Fig. 4E). The density of xanthophores in the dorsal region of *mc1r*$^{K.O.}$ mutants was lower than in WT fish. However, the density of xanthophores in the ventral regions of *mc1r*$^{K.O.}$ fish was considerably higher than in WT fish (Fig. 4F).

We also compared the distribution of transgenic markers for melanophores and iridophores in *mc1r*$^{K.O.}$ mutants and their WT siblings to assess densities of possible unpigmented pigment cells or their precursors. Firstly, we imaged fish carrying the Tg(Kita:GalTA4,UAS:mCherry) transgene, which labels melanophores with membrane-bound mCherry (Anelli et al., 2009). WT fish showed no pigmented melanophores in the ventral skin (Fig. 5A, B), but there were also no unpigmented mCherry-expressing cells suggesting a complete absence of melanophores and melanoblasts (Fig. 5B). In contrast, *mc1r*$^{K.O.}$ mutants showed an increase in mCherry labelled melanophores in the ventral skin region (Fig. 5C, D). This is in agreement with the detected increase in the number of melanophores in ventral regions (Fig. 4). By analyzing fish carrying Tg(TDL358:GFP), a transgene labeling iridophores and glia with cytosolic GFP (Levesque et al., 2013), we confirmed the presence of a dense and uniform sheet of iridophores in the ventral abdominal skin of WT fish (Figs. 5E,

F) and showed that this layer is broken up into smaller fragments in *mc1r*$^{K.O.}$ mutants (Fig. 5G, H). Although it is difficult to quantify the contribution of changed cell numbers to this phenotype, *mc1r*$^{K.O.}$ mutants display a significant reduction of the extent of iridophores, together with a significantly increased number of melanophores and xanthophores (Fig. 5G) within the ventral abdominal skin.

Finally, we characterized the contribution of pigment cells in the scales to the disrupted countershading and pale phenotype in *mc1r*$^{K.O.}$ mutants. Scales isolated from the dorsum of *mc1r*$^{K.O.}$ mutants displayed a substantial reduction of melanophores (Fig. 6B, black arrowheads) compared to WT fish (Fig. 6A). In contrast to ventral scales of WT siblings which lack all pigmented cell-types (Fig. 6C), ventral scales from *mc1r*$^{K.O.}$ mutants display some ectopic melanophores (Fig. 6D, black arrowheads) and numerous xanthophores (Fig. 6D, yellow arrowheads).

Zebrafish Asip1 is likely acting as an inverse agonist of Mc1r

To determine if Asip1 signaling is mediated by Mc1r, we analyzed the combination of *mc1r*$^{K.O.}$ with the *asip1*-Tg zebrafish line that overexpresses *asip1* in the entire body. We predicted that, if Asip1 signaling functions solely through Mc1r that the *mc1r*$^{K.O.}$/ *asip1*-Tg fish would show a pattern identical to the *mc1r*$^{K.O.}$ line, whereas if another receptor contributed to Asip1 signaling, the pattern would be more similar to the *asip1*-Tg line. Both *mc1r*$^{K.O.}$ and *asip1*-Tg zebrafish lines differ significantly in their overall pigmentation phenotype compared to WT fish (Fig. 7). WT fish (Fig. 7A) show a specific striped pattern (Fig. 7 B), a light ventrum (Fig. 7C) and a darker dorsum (Fig. 7D). In *mc1r*$^{K.O.}$ mutants (Fig. 7E) the striped pattern is barely affected (Fig. 7F), but they show a darker belly (Fig. 7G) and a paler dorsum with fewer melanophores than WT fish (Fig. 7 H,R). The *asip1*-Tg zebrafish phenotype presents a slightly affected

striped pattern (Fig 7J), a light belly similar to WT fish (Fig. 7K), but a drastic reduction of dorsal melanophores (Fig. 7L,S) due to the ectopic overexpression of *asip1* (Ceinos et al., 2015). In the combination of *mc1r*$^{K.O.}$ with *asip1*-Tg, the *asip1*-Tg phenotype is suppressed and the *mc1r*$^{K.O.}$ phenotype prevails (Fig. 7M). The *mc1r*$^{K.O.}$ + *asip1*-Tg zebrafish line presented the same barely affected stripe pattern like *mc1r*$^{K.O.}$ alone (Fig. 7 N), the pigmented belly (Fig. 7O) and the dark dorsum with similar numbers of melanophores as the *mc1r*$^{K.O.}$ fish (Fig. 7P,T). Fish overexpressing *asip1* are paler than fish lacking Mc1r. This suggests that Asip1 has additional effects to those promoted by Mc1r, either by competitive antagonism or inverse agonism, as the overexpression phenotype is stronger than absence of the receptor. Fish that overexpress Asip1 but also lack Mc1r have a ventrally dorsalized pigmentation phenotype, similar to fish only lacking Mc1r, indicating that Asip1 is probably acting as an inverse agonist of Mc1r to elicit the opposite response from that produced by α-Msh. Additionally, scales isolated from the dorsum of the *mc1r*$^{K.O.}$/ *asip1*-Tg fish displayed a similar substantial reduction of melanophores than *mc1r*$^{K.O.}$ mutants (Fig. S1A,C) compared to WT fish (Fig. 6A) and an increase of melanophores compared to *asip1*-Tg fish (Fig.S1B) . Ventral scales from *mc1r*$^{K.O.}$/ *asip1*-Tg also showed some melanophores and numerous xanthophores (Fig. S1F).

DISCUSSION

Zebrafish, a major teleost fish model for pigmentation studies, utilizes two distinct mechanisms to generate the adult pigmentation, the striped patterning and the dorso-ventral countershading mechanism (Ceinos et al., 2015). Both mechanisms function largely independently, with the resultant patterns superimposed to give the full pattern (Ceinos et al., 2015). The dorso-ventral expression gradient of *asip1* is responsible for

the countershading, through inhibition of melanogenesis in the ventral region where *asip1* is highly expressed. However, Asip1 is also involved in the regulation of chromatophore numbers since its overexpression modifies the melanophore/iridophore ratio by promoting iridophore differentiation in absence of melanophores (Ceinos et al., 2015). Our previous studies have demonstrated that Asip1 works as a competitive antagonist of both Mc1r and Mc4r (Cerdá-Reverter et al.,2005; Guillot et al., 2016) but likely also as an inverse agonist of the constitutively activated Mc1r (Guillot et al., 2016; Sánchez et al., 2010). *Asip1* overexpression in zebrafish results in a ventralization of the dorsal skin pigmentation due to a substantial reduction in the number of melanophores and the concomitant production of extra iridophores, without effects on the ventral pigmentation (Ceinos et al., 2015). In blind Mexican cave tetra (*Astyanax mexicanus*) Mc1r plays a key role in the establishment of the adult pigment pattern; inactivating mutations are responsible for the reduction in the number of melanophores, a phenotype that can be recapitulated in zebrafish by *mc1r* morpholino knockdown (Gross et al., 2009).We now demonstrate that inactivating mutations of *mc1r* in zebrafish lead to a reduction in the number of dorsal melanophores, and that also extends to the dorsalmost stripe. In addition they lead to a significant reduction in the number of dorsal xanthophores during all post-metamorphic stages studied. If Asip1 works as an inverse agonist of the constitutively activated Mc1r, inactivating mutations of the cognate receptor would be predicted to recapitulate the *asip1-Tg* dorsal effect. However, the number of dorsal melanophores in *asip1-Tg* fish was less reduced in an $mc1r^{K.O.}$ background when compared to a WT background. Also, *asip1-Tg* zebrafish exhibit an extra dorsal band of iridophores (Ceinos et al., 2015), which is absent in $mc1r^{K.O.}$ mutants. Therefore, overexpression of *asip1* in $mc1r^{K.O.}$ background yields a similar phenotype to that of *mc1r* knockout mutant unmasking what is

essentially an epistatic relationship between asip1 and mc1r. Our data demonstrate that Asip1 displays a more pronounced effect when Mc1r is present and suggests that the effect is more than simply blocking of the constitutive activity of Mc1r (Ollmann et al., 1998). Similar results have been reported in mouse showing that individuals ubiquitously expressing high levels of *asip* exhibit paler yellow fur than that seem when *mc1r* is absent (Ollmann et al., 1998; Jackson et al., 2007).

The dorsal root ganglia (DRG) host multipotent stem cells that can generate all three pigment-cell types found in the post-metamorphic skin of zebrafish (Singh et al., 2016). These stem cells remain multipotent until well into metamorphosis when individual pigment cell fates become specified (Singh et al., 2016). Under our original model, the constitutive or MSH-induced activation of Mc1r promotes melanocyte fate decisions and differentiation in the dorsal skin, but in the more ventral regions, the inverse agonism or competitive antagonism of Asip1 would block Mc1r activity, instead promoting the differentiation of iridophores. Accordingly, we would expect the phenotype of the *asip1-Tg* line (where Mc1r inactivation is driven by dorsal overexpression of *asip1*) to be similar to the phenotype of the $mc1r^{K.O.}$ line (where all Mc1r is eliminated by mutation). As discussed above both dorsal phenotypes (*asip1-Tg* vs $mc1r^{K.O.}$) differed extensively thus challenging this original hypothesis. Our results suggest that melanophore lineage specification and differentiation in the dorsal skin are not fully dependent on Mc1r activity and thus, some other receptors, presumably other Mcrs, interact with Asip1. The presence of different Mcrs has been reported in several species (see introduction for references). However, we cannot exclude that some other non-melanocortin receptors could be involved in Asip1 function, since Agouti is able to increase intracellular Ca^{2+} levels in skeletal myocytes via mechanisms that may not involve Mcr antagonism (Zemel et al., 1995). In mice, it

has been suggested that the stronger pheomelanic phenotype of asip overexpressing mice carrying mc1r mutation might result from a β-arrestin-mediated mechanism leading to increased cAMP degradation, reducing the signaling to greater level than when mc1r is absent (Jackson et al., 2007). Such a mechanism would also be conceivable here in zebrafish.

Our data suggest that most precursors in the dorsal region need an Asip1-free environment to become melanophores but the *mc1r*$^{K.O.}$ phenotype suggests that only some of them seem to require a functional Mc1r. However, the *mc1r*$^{K.O.}$*+asip1-Tg* phenotype is similar to the *mc1r*$^{K.O.}$ phenotype, suggesting that the inhibitory effects of Asip1 on melanophores require a functional Mc1r.

We note that only the melanophores along the dorsal midline are apparently resistant to the presence of high Asip1 levels (see schematic representation on Fig. 8). However, these melanophores are distinct in that they are localized immediately dorsal to the CNS and not in the skin; these dorsal midline cells might be insensitive to Asip1, for example, because they lack *mc1r* expression. Consistent with this explanation, we note that these dorsal midline melanophores are unaffected in *mc1r* mutants and the *mc1r*$^{K.O}$*;Asip1-Tg* combination. Furthermore, our observations indicate that these cells are likely to derive from persisting embryonic melanocytes of the early larval dorsal stripe, rather than from adult pigment stem cells. Alternatively, a trivial explanation of the difference might be that the *Asip1-Tg* shows less robust expression of *Asip1* in the adjacent tissues (CNS and/or dorsal myotome).

In contrast to the dorsal region, the effects of Mc1r dysfunction in the ventral region depend on the developmental stage. During the early post-metamorphic stages, Mc1r knockout induces similar effects to those observed in the dorsal region, i.e. a decrease in the density of melanophores. However, in adult animals, the effects are opposite to

455 those observed in the dorsal area or during the early post-metamorphic stages in the
456 ventral skin. This we interpret as a dorsalisation of the ventral region. Therefore,
457 functional Mc1r is necessary to block melanophores and xanthophores in favor of
458 iridophores in the ventral skin of adult animals. Ventral Asip1 levels would limit
459 melanophore/xanthophore specification, differentiation and/or proliferation and
460 conversely promote iridophores, but since this pathway requires the expression of
461 *mc1r*, its absence in the mutants will allow the production of ventral melanophores and
462 xanthophores and result in a reduction in the iridophore number. This dorsalisation
463 phenomenon of the ventral region extends also to the ventral-most stripes, with a
464 thickened 2V-stripe and a fully-developed 3V-stripe in the ventrum of $mc1r^{K.O.}$ mutant
465 lines. Therefore, Asip1-induced inhibition of melanogenesis and melanophore
466 differentiation *via* Mc1r may limit the addition of new dark stripes in the ventral
467 region.
468 Finally, we also analyzed the effect of Mc1r dysfunction in the dorsal and ventral
469 scales. As expected, ventral scales in WT fish lack all chromatophores but the absence
470 of a functional Mc1r results in the development of ectopic melanophores and numerous
471 xanthophores, again consistent with our interpretation of this dorsalisation of the
472 ventral skin. However, the effect on dorsal scales was slightly different from that
473 observed in the dorsal skin. Dorsal scales exhibit a reduction in the number of
474 melanophore similar to that recorded in the dorsal skin but the number of xanthophores
475 is increased dramatically. Further work will be necessary to understand the different
476 responses to Mc1r absence of these progenitors in scales versus the skin.
477 In summary, we demonstrate that Mc1r is involved in the establishment of the dorso-
478 ventral pigment pattern in zebrafish. The ventral region requires a functional Mc1r to
479 block the production of melanophores and xanthophores and to promote iridophores.

In the dorsal region, the absence of Mc1r only results in a partial reduction in the number of melanophores and xanthophores suggesting the potential involvement of additional Mcrs in mediating the antagonistic signal of Asip1.

ACKNOWLEDGEMENTS

We thank Christiane Nüsslein-Volhard Lab from Max-Planck Institute (Germany) for providing the TDL358:GFP and Kita:GalTA4;UAS:mCherry transgenic lines. We would also like to thank Inés Pazos Garridos (CACTI, University of Vigo, Spain) for her assistance with confocal imaging and Pili Comesaña for her help in handling and care of the fish. This work was funded by the Spanish Economy and Competitiveness Ministry projects AGL2011-23581, AGL2014-52473R, AGL2017-89648P to JR. Partial funding was obtained from AGL2016-74857-C3-3-R to JMCR. L. Cal was supported by pre-doctoral fellowship FPI funded by Spanish Economy and Competitiveness Ministry (AGL2011-23581) and by pre-doctoral fellowship of the Spanish Personnel Research Training Program funded by Spanish Economy and Competitiveness Ministry (EEBB-C-14- 00467). P Suarez-Bregua was supported by AGL2014-52473R and AGL2017-89648P project contract. The funders had no role in study design, data collection and analysis, decision to publish or preparation of the manuscript. None of the contributing authors has any competing interests.

REFERENCES

Aberdam, E., Bertolotto, C., Sviderskaya, E.V., de Thillot, V., Hemesath, T.J., Fisher, D.E., Bennett, D.C., Ortonne, J.P. and Ballotti, R. (1998) Involvement of microphthalmia in the inhibition of melanocyte lineage differentiation and of melanogenesis by agouti signal protein. *J Biol Chem* **273**, 19560–19565.

505 Agulleiro, M., Sánchez, E., Leal, E., Cortés, R., Fernández-Durán, B., Guillot, R.,
506 Davis, P., Dores, R.M., Gallo-Payet, N. and Cerdá-Reverte, J.M. (2013) Molecular
507 characterization and functional regulation of melanocortin 2 receptor (MC2R) in
508 the sea bass. A putative role in the adaptation to stress. *PLoS One* **8**, e65450.

509 Anelli, V., Santoriello, C., Distel, M., Köster, R.W., Ciccarelli, F.D. and Mione M.
510 (2009) Global repression of cancer gene expression in a zebrafish model of
511 melanoma is linked to epigenetic regulation. *Zebrafish* **6**, 417–424.

512 Bassett, A.R., Tibbit, C., Ponting, C.P. and Liu, J.L. (2013) Highly Efficient
513 Targeted Mutagenesis of Drosophila with the CRISPR/Cas9 System. *Cell Rep* **4**,
514 220–8.

515 Cal, L., Megías, M., Cerdá-reverter, J. , Postlethwait. J.H., Braasch, I. and Rotllant,
516 J. (2017) BAC Recombineering of the Agouti Loci from Spotted Gar and Zebrafish
517 Reveals the Evolutionary Ancestry of Dorsal–Ventral Pigment Asymmetry in Fish.
518 *J Exp Zool Part B Mol Dev Evol* **328**, 697–708.

519 Cal, L., Suarez-Bregua, P., Comesaña, P., Owen, J., Braasch, I., Kelsh, R., Cerdá-
520 Reverter, J.M., Rotllant J. (2019)Countershading in zebrafish results from an
521 Asip1 controlled dorsoventral gradient of pigment cell differentiation. *Sci Rep***.**
522 **9**(1):3449. doi: 10.1038/s41598-019-40251-z.

523 Ceinos, R.M., Guillot, R., Kelsh, R.N., Cerdá-Reverter, J.M. and Rotllant, J.
524 (2015) Pigment patterns in adult fish result from superimposition of two largely
525 independent pigmentation mechanisms. *Pigment Cell Melanoma Res* **28**, 196–209.

526 Cerdá-Reverter, J..M, Agulleiro, M.J., Cortés, R., Sánchez, E., Guillot, R., Leal,
527 E., Ferández-Durán, B., Puchol, S. and Eley, M. (2013) Involvement of
528 melanocortin receptor accessory proteins (MRAPs) in the function of
529 melanocortin receptors. *Gen Comp Endocrinol* **188**:133-6 doi:
530 10.1016/j.ygcen.2013.01.017.

531 Cerdá-Reverter, J.M., Haitina, T., Schiöth, H.B. and Peter, R.E. (2005) Gene
532 Structure of the Goldfish Agouti-Signaling Protein: A Putative Role in the Dorsal-
533 Ventral Pigment Pattern of Fish. *Endocrinology* **146**, 1597–1610.

534 Cerdá-Reverter, J.M., Ling, M.K., Schiöth, H.B. and Peter, R.E. (2003) Molecular
535 cloning, characterization and brain mapping of the melanocortin 5 receptor in the
536 goldfish. *J Neurochem* **87**, 1354–1367.

537 Cerdá-Reverter, J.M., Ringholm, A., Schiöth, H.B. and Peter, R.E. (2003)
538 Molecular cloning, pharmacological characterization, and brain mapping of the
539 melanocortin 4 receptor in the goldfish: involvement in the control of food intake.
540 *Endocrinology* **144**, 2336–2349.

541 Cortés, R., Navarro, S., Agulleiro, M.J., Guillot, R., García-Herranz, V., Sánchez,
542 E. and Cerdá-Reverter, J.M. (2014) Evolution of the melanocortin system. *Gen*
543 *Comp Endocrinol* **209**:3-10. doi: http://dx.doi.org/10.1016/ j.ygcen.2014.04.005

544 Gross, J.B., Borowsky, R. and Tabin, C.J. (2009) A novel role for Mc1r in the
545 parallel evolution of depigmentation in independent populations of the cavefish
546 Astyanax mexicanus. *PLoS Genet* **5**, e1000326.

547 Guillot, R., Ceinos, R.M., Cal, R., Rotllant, J. and Cerdá-Reverter, J.M. (2012)
548 Transient ectopic overexpression of agouti-signalling protein 1 (Asip1) induces
549 pigment anomalies in flatfish. *PLoS One* **7**, e48526.

550 Guillot, R., Corté,s R., Navarro, S., Mischitelli, M., García-Herranz, V.,, Sánchez,
551 E., Ca,l L., Navarro, J.C., Míguez, J.M., Afanasyev, S., Krasnov, A., Cone, R.D.,
552 Rotllant, J. and Cerdá-Reverter, J.M. (2016) Behind melanocortin antagonist
553 overexpression in the zebrafish brain: A behavioral and transcriptomic approach.
554 *Horm Behav* **82**, 87–100.

555 Hirata, M., Nakamura, K., Kanemaru, T., Shibata, Y. and Kondo, S. (2003)
556 Pigment cell organization in the hypodermis of zebrafish. *Dev Dyn* **227**, 497–503.

557 Hirata, M., Nakamura, K.I. and Kondo, S. (2005) Pigment cell distributions in
558 different tissues of the zebrafish, with special reference to the striped pigment
559 pattern. *Dev Dyn* **234**, 293–300.

560 Jackson, I.J., Budd, P.S., Keighren, M., McKie, L. (2007)
561 Humanized MC1R transgenic mice reveal human specific receptor function. Hum
562 Mol Genet. **16**(19):2341-8.

563 Kelsh, R.N. (2004) Genetics and evolution of pigment patterns in fish. *Pigment*
564 *Cell Res* **17**, 326–336.

565 Kimmel, C.B., Ballard, W.W., Kimmel, S.R., Ullmann, B. and Schilling, T.F.
566 (1995) Stages of embryonic development of the zebrafish. *Dev Dyn* **203**, 253–310.

567 Kobayashi, Y., Mizusawa, K., Saito, Y. and Takahashi, A. (2012) Melanocortin

568 systems on pigment dispersion in fish chromatophores. *Front Endocrinol* 3(**9**), 1-
569 6.

570 Kottler, V.A., Künstner, A. and Schartl, M. (2015) Pheomelanin in fish? Pigment
571 *Cell Melanoma Res* **28**, 355–356.

572 Le Pape, E., Passeron, T., Giubellino, A., Valencia, J.C., Wolber, R. and Hearing,
573 V.J. (2009) Microarray analysis sheds light on the dedifferentiating role of agouti
574 signal protein in murine melanocytes via the Mc1r. *Proc Natl Acad Sci U S A* **106**,
575 1802–1807.

576 Levesque, M.P., Krauss, J., Koehler, C., Boden, C. and Harris, M.P. (2013) New
577 Tools for the Identification of Developmentally Regulated Enhancer Regions in
578 Embryonic and Adult Zebrafish. *Zebrafish* **10**, 21–29.

579 Linnen, C., Poh, Y., Peterson, B., Barret., R, Larson, J., Jensen, J. and Hoekstra,
580 H.E. (2013) Adaptive evolution of multiple traits throug multiple mutations at a
581 single gene. *Science* **339**, 1312–1316.

582 Michaud, E.J., Bultman, S.J., Stubb,s L.J, and Woychik, R.P. (1993) The
583 embryonic lethality of homozygous lethal yellow mice AylAy] is associated with
584 the disruption of a novel RNA-binding protein. *Genes Dev***. 7**, 1203–1213.

585 Miller, M.W., Duhl, D.M., Vrieling, H., Cordes, S.P., Ollmann, M.M., Winkes,
586 B.M. and Barsh, S. (1993) Cloning of the mouse agouti gene predicts a secreted
587 protein ubiquitously expressed in mice carrying the lethal yellow mutation. *Genes*
588 *Dev* **7**, 454–467.

589 Montague, T.G., Cruz, J.M., Gagnon, J., Church, G.M. and Valen, E. (2014)
590 CHOPCHOP: a CRISPR/Cas9 and TALEN web tool for genome editing. *Nucleic*
591 *Acids Res* **42**:401-7. doi: 10.1093/nar/gku410

592 Ollmann, M.M., Lamoreux, M.L., Wilson, B.D., Barsh, G.S. (1998) Interaction of
593 Agouti protein with the melanocortin 1 receptor in vitro and in vivo. *Genes Dev* **12**
594 (3): 316-30.

595

596 Parichy, D.M., Elizondo, M.R., Mills, M.G., Gordon, T.N. and Engeszer, R.E.
597 (2009) Normal table of postembryonic zebrafish development: Staging by
598 externally visible anatomy of the living fish. *Dev Dyn* **238**, 2975–3015.

599 Robbins, L.S., Nadeau, J.H., Johnson, K.R., Kelly, M.A., Roselli-Rehfuss, L.,
600 Baack, E., Mountjoy, K.G. and Cone, R.D. (1993) Pigmentation phenotypes of
601 variant extension locus alleles result from point mutations that alter MSH receptor
602 function. *Cell* **72**(6):827–34.

603 Sánchez, E., Rubio, V.C. and Cerdá-Reverter, J.M. (2009) Characterization of the
604 sea bass melanocortin 5 receptor: a putative role in hepatic lipid metabolism. *J Exp*
605 *Biol* **212**, 3901–3910.

606 Sánchez, E., Rubio, V.C. and Cerdá-Reverter, J.M. (2010) Molecular and
607 pharmacological characterization of the melanocortin type 1 receptor in the sea
608 bass. *Gen Comp Endocrinol* **165**, 163–169.

609 Schiöth, H.B., Haitina, T., Ling, M.K., Ringholm, A., Fredriksson, R., Cerdá-

610 Reverter, J.M. and Klovins, J. (2005) Evolutionary conservation of the structural,
611 pharmacological, and genomic characteristics of the melanocortin receptor
612 subtypes. *Peptides* **26**, 1886–1900.

613 Singh, A.P., Dinwiddie, A., Mahalwar, P., Schach, U., Linker, C., Irion, U. and
614 Nüsslein-Volhard, C. (2016) Pigment Cell Progenitors in Zebrafish Remain
615 Multipotent through Metamorphosis. *Dev Cell* **38**, 316–330.

616 Sviderskaya, E.V., Hill, S.P., Balachandar, D., Barsh, G.S. and Bennett, D.C.
617 (2001) Agouti signaling protein and other factors modulating differentiation and
618 proliferation of immortal melanoblasts. *Dev Dyn* **221**, 373–379.

619 Vrieling, H., Duhl, D.M., Millar, S.E., Miller, K. and Barsh, G.S. (1994)
620 Differences in dorsal and ventral pigmentation result from regional expression of
621 the mouse agouti gene. *Pro.c Natl. Acad. Sci. U S A.* **91**, 5667–5671.

622 Wei, R., Yuan, D., Zhou, C., Wang, T., Lin, F., Chen, H., Wang, Y., Liu, J., Gao,
623 Y. and Li, Z. (2013) Cloning, distribution and effects of fasting status of
624 melanocortin 4 receptor (MC4R) in Schizothorax prenanti. *Gene* 532, 100–107.

625 Westerfield, M. (2007) *The Zebrafish Book. A Guide for the Laboratory Use of*
626 *Zebrafish (Danio rerio).* 5th edn. University of Oregon Press, Eugene

627 Zemel, M.B., Kim, J., Woychikt, R.P., Michaudt, E.J., Kadwellt, S., Patelt, I.R.
628 and Wilkison, W.O. (1995) Agouti regulation of intracellular calcium : Role in the
629 insulin resistance of viable yellow mice. *Proc Natl Acad Sci* **92**, 4733–4737.

630

FIGURE LEGENDS

Figure 1. CRISPR/Cas9-induced mutations in the zebrafish *mc1r* gene. (A) Scheme of the *mc1r* single exon gene showing the target sites (black arrowheads: T1, T2). Coding region (CDS) are represented as white boxes and 5' UTR and 3'UTR are shown as black boxes. (B) Sequence of induced mutations in the *mc1r* gene. The first and fourth lines show the wild-type target sequences (T1 and T2). Black arrowheads label the protospacer-adjacent motif (PAM). The following lines show different induced mutations. Italic lower case letters represent inserted new sequence. The number of deleted (-) and inserted (+) bases are marked in the right side of each sequence. Selected mutations for further analysis are labeled by white arrowheads. (C) Predicted amino acid sequence encoded by generated *mc1r* variants. The first line shows the wild type protein, and following lines show the potential protein sequence of each selected mutation. Grey boxes show part conserved with the wild type (WT) sequence. Asterisk represents the stop codon. Mutation M2 generates the shortest predicted protein.

Figure 2. The adult dorsal-ventral countershading pattern is disrupted in *mc1r*$^{K.O}$
Lateral (A, B), anterior-lateral (C, D), ventral-head (E, F), ventral-belly (G, H) and dorsal (I, J) views of 210 dpf WT and *mc1r*$^{K.O}$ zebrafish. (A, B) The pigment pattern of WT zebrafish is a striped pigment pattern with dark stripes and light interstripes. Each dark stripe has a standard nomenclature: two primary stripes are called 1D and 1V, and the two secondary stripes are named 2D and 2V. The *mc1r*$^{K.O}$ phenotype is characterized by a darker ventrum than WT. (C, D) The striped pigment pattern looks almost unaltered in *mc1r*$^{K.O}$ fish. The only perceptible modification is that the *mc1r*$^{K.O.}$ mutant fish showed a thickened 2V-stripe and a fully-developed 3V-stripe in the

ventrum compared to WT. The darker ventrum of *mc1r*$^{K.O}$ than WT fish is clearly evident. (E, F) In WT, the melanophores appear in reduced numbers around the jaws and branchiostegals; however, branchiostegal, jaw and operculum regions are hyperpigmented in *mc1r*$^{K.O.}$. (G, H) Melanophores on the WT belly are virtually absent; thus, their ventral region shows a bright white color as a result of high numbers of iridophores in the abdominal wall. However, *mc1r*$^{K.O}$ shows hyperpigmentation, with increased numbers of melanophores and xanthophores in ventral skin, and the abdominal wall seems to be also affected because it appears overall more yellowish than WT. (I, J) The dorsal region is also affected in *mc1r*$^{K.O.}$: the WT dorsum shows more melanophores than the *mc1r*$^{K.O}$ dorsum. Scale bar: (A,B) 5 mm, (C,D, E, F, G, H) 1 mm and (I, J) 0.5 mm. Abbreviation: br, branchiostegal.

Figure 3. Dorsal-ventral distribution of melanophores during metamorphosis. (A) Distribution and density of melanophores in WT and *mc1r*$^{K.O.}$ 15dpf fish. At this stage, *mc1r*$^{K.O}$ shows significantly lower density of melanophores in the dorsal region, lateral region and in the belly. (B) Distribution and density of melanophores in WT and *mc1r*$^{K.O}$ 30 dpf fish. At this stage, *mc1r*$^{K.O}$ shows significantly lower density of melanophores in the dorsal region of the head, in the dorsal region, in the lateral region, and in the belly region. Data are the mean±SEM, n=6 fish. Asterisks indicate significant differences between WT and *mc1r*$^{K.O}$ fish. Scale bar: (A) 200 μm, (B) 500 μm.

Figure 4. Dorsal-ventral distribution of melanophores and xanthophores in WT and *mc1r*$^{K.O}$ adult fish. (A) Lateral view of zebrafish showing the body regions selected for melanophore and xanthophore count at 210dpf. (B) Ventral view of bellies of WT and *mc1r*$^{K.O.}$ zebrafish at 210 dpf . (C) Distribution and density of melanophores in 60 dpf WT and *mc1r*$^{K.O}$ fish. At this stage, *mc1r*$^{K.O}$ shows significantly lower density of melanophores in dorsal head, dorsal region, and black stripes 2D, 1D and 1V.

However, *mc1r*$^{K.O}$ shows significantly higher density of melanophores in the ventral region of the head. (D) Density of xanthophores in dorsal and ventral skin of WT and *mc1r*$^{K.O}$ 60 dpf fish. At this stage, *mc1r*$^{K.O}$ shows significantly higher density of xanthophores in the belly region. (E) Distribution and density of melanophores in WT and *mc1r*$^{K.O}$ 210 dpf fish. At this stage, *mc1r*$^{K.O.}$ shows significantly lower density of melanophores in dorsal head, dorsal region and black stripes 2D and 1D; conversely, *mc1r*$^{K.O.}$ shows significantly higher density of melanophores in black stripe 3V, ventral head and belly. (F) Number of xanthophores in dorsal and ventral skin of WT and *mc1r*$^{K.O}$ 210 dpf fish. The *mc1r*$^{K.O}$ fish showed highly significant lower density of xanthophores in dorsal regions and significantly higher density of xanthophores in belly region than WT. Data are the mean ±SEM, n=7. Asterisks indicate significant differences between WT and *mc1r*$^{K.O}$ fish. Scale bar (A,C,E) 1mm, (B) 100 μm.

Figure 5. Detection of transgenically-labelled pigment cells in WT and *mc1r*$^{K.O}$ fish. (A) Ventral view of 210 dpf WT belly. (B) Belly of 210 dpf WT fish carrying Tg(Kita:GalTA4;UAS:mCherry) transgene shows no melanophores in ventral skin. (C) Ventral view of 210 dpf *mc1r*$^{K.O}$ belly. (D) Belly of 210 dpf *mc1r*$^{K.O}$ fish carrying Tg(Kita:GalTA4;UAS:mCherry) transgene shows higher number of melanophores in ventral skin (white arrow). (E) Internal view of 210 dpf fish abdominal wall. WT ventral abdominal wall shows a white sheet of iridophores with few internal melanophores (black arrow). (F) Ventral abdominal wall of 210 dpf WT fish carrying Tg(TDL358:GFP) transgene displays a uniform sheet of iridophores. (G) Ventral abdominal wall of 210 dpf *mc1r*$^{K.O}$ shows a discontinuous sheet of iridophores with high number of melanophores. (H) Ventral abdominal wall of 210 dpf *mc1r*$^{K.O}$ fish

carrying Tg(TDL358:GFP) transgene exhibits a broken sheet of iridophores. Scale bars: 100 μm.

Figure 6. Adult *mc1r*$^{K.O}$ dorsal and ventral scales displayed an anomalous color pattern. (A) A typical 210 dpf WT dorsal scale exhibit a pattern of melanophores (black arrowheads) and xanthophores (yellow arrowheads). (B) 210 dpf *mc1r*$^{K.O}$ dorsal scale exhibits a strong reduction of melanophores number (black arrowheads). (C) A typical 210 dpf WT ventral scale does not exhibit any chromatophores. (D) 210 dpf *mc1r*$^{K.O}$ ventral scales exhibit a pattern of melanophores (black arrowheads) and xanthophores (yellow arrowheads). Scale bars: 100 μm.

Figure 7. Interaction between *asip1* overexpression phenotype and *mc1r*$^{K.O}$ fish. Lateral (A, E, I, M), anterior-lateral (B, F, J, N), ventral-belly (C, G, K, O) and dorsal (D, H, L, P) views of 100 dpf WT, *mc1r*$^{K.O.}$, *asip1*-Tg zebrafish and *mc1r*$^{K.O}$+*asip1*-Tg. (A) The pigment pattern of WT zebrafish shows (B) normal striped pattern, (C) light belly, and (D) dark dorsum. (E) The pigment pattern of *mc1r*$^{K.O}$ fish shows (F) almost normal striped pattern with a dark stripe 3V more developed and the dark stripe 2D less developed than WT fish, (G) hyperpigmented belly, and (H) a lesser pigmented dorsum compared to WT. (I) The pigment pattern of *asip1*-Tg fish shows (J) almost normal striped pattern, but without dark stripe 2D, (K) light belly, and (L) hypopigmented dorsum. (M) The *mc1r*$^{K.O}$+*asip1*-Tg phenotype shows the same phenotype as the *mc1r*$^{K.O}$ phenotype. Almost normal striped pattern with a dark stripe 3V (N) more developed and the dark stripe 2D less developed than WT fish, (O) hyperpigmented belly and (P) a lesser pigmented dorsum. (Q-T) Density of melanophores in dorsal and the ventral region of WT (Q), *mc1r*$^{K.O.}$(R), *asip1*-Tg (S)

733 and *mc1r*$^{K.O}$+*asip1*-Tg (T) adult fish. Data are the mean±SEM, n=6 fish. Scale bar: (A,
734 E, I, M) 2 mm, (B, C, D, F, G, H, J, K, L, N, O, P) 1 mm.
735
736 **Figure 8**: **Schematic representation of melanophore dorsal phenotypes of WT,**
737 ***mc1r*$^{K.O}$, *asip1-Tg* and *mc1r*$^{K.O.}$+*asip1-Tg* fish.** We propose three different
738 melanophore cohorts in the dorsal skin of adult fish: Mc1r-free melanophores (❁,also
739 called Asip1-independent), melanophores expressing Mc1r (●, also call Mc1r-
740 dependent), melanophores expressing Mc1r but also expressing a second Mcr (●, also
741 called Mc1r-independent melanophores). The sum of melanophore populations
742 expressing only Mc1r together with the melanophores that express Mc1r together with
743 another Mcr are called Asip-1 dependent melanophores (see text for more
744 information).

SUPPLEMENTARY DATA

Figure S1. Functional Asip1/Mc1r interaction on dorsal (upper row) and ventral (lower row) scales color pattern in adult fish. (A) *mc1r*$^{K.O}$ dorsal scales exhibits a reduction of melanophores and xanthophore number compared to the typical adult WT fish dorsal scales. (B) *asip1-Tg* dorsal scale exhibits a substantial reduction of melanophores and xanthophore number compared to the *mc1r*$^{K.O}$ dorsal scales and the typical adult WT dorsal scales color pattern. (C) *mc1r*$^{K.O}$*+asip1-Tg* dorsal scales exhibits a melanophores and xanthophore number similar to that shown by the *mc1r*$^{K.O}$ dorsal scales. (D) *mc1r*$^{K.O}$ ventral scales exhibit a pattern of melanophores and xanthophores. (E) Asip1-Tg ventral scale does not exhibit any chromatophores, similar to the typical ventral scale of adult WT fish. (F) *mc1r*$^{K.O}$*+asip1-Tg* ventral scales exhibit a pattern of melanophores and xanthophores similar to that shown by the *mc1r*$^{K.O}$ ventral scales. Scale bars: 100 μm.

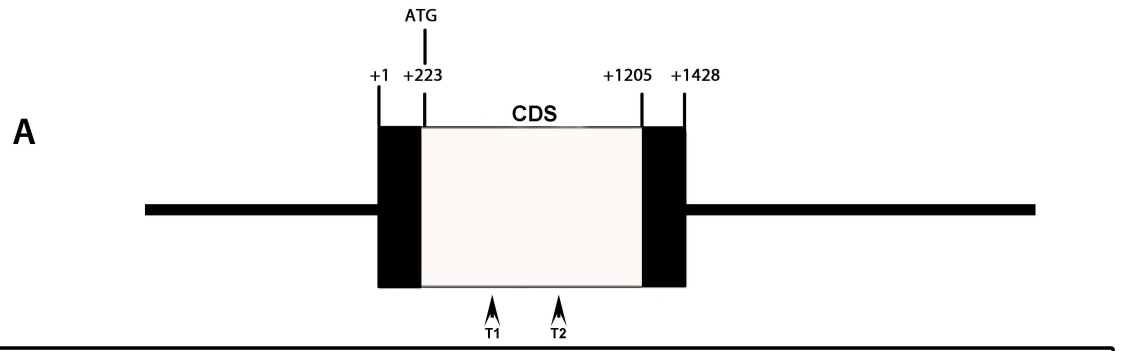

B

Target (T1)

WT> CGGTGGCAGACATGCTAGTGAGCGTCAGTA----ATGTGGTGGAGACGTTGTTTATG

M1> CGGTGGCAGACATGCTAGTGAGCGTCAGTA*tca*ATGTGGTGGAGACGTTGTTT (+3)

M2> CGGTGGCAGACATGCTAGTGAGCGTCAGTA*ggtgtggtgga* GGAGACGTTGTTT (-7;+11)

Target (T2)

WT> GGTTCTGTACCTGCACA---------- TGTTCATCTTGGCCCATGTCCACTCAA

M3> GGTTCTGTACCTGCA---------- TGTTCATCTTGGCCCATGTCCACTCAA (-2)

M4> GGTTCTGTACCTGCA*tctgctcataaaaatc*TGTTCATCTTGGCCCATGTCCACTCAA (-2;+16)

M5> GGTT---------- CA----------TGTTCATCTTGGCCCATGTCCACTCAA (-11)

M6> GGTTCTGTACCTG---------- TTCATCTTGGCCCATGTCCACTCAA (-6)

C

WT> MNDSSRHHFSMKHMDYMYNADNNITLNSNSTASDINVTGIAQIMIPQELFLMLG
M2> MNDSSRHHFSMKHMDYMYNADNNITLNSNSTASDINVTGIAQIMIPQELFLMLG
M3> MNDSSRHHFSMKHMDYMYNADNNITLNSNSTASDINVTGIAQIMIPQELFLMLG
M4> MNDSSRHHFSMKHMDYMYNADNNITLNSNSTASDINVTGIAQIMIPQELFLMLG

WT> LISLVENILVVVAIIKNRNLHSPMYYFICCLAVADMLVSVSNVVETLFMLLTEHGLLL
M2> LISLVENILVVVAIIKNRNLHSPMYYFICCLAVADMLVSVSRCGGGDVVYVTDGAW
M3> LISLVENILVVVAIIKNRNLHSPMYYFICCLAVADMLVSVSNVVETLFMLLTEHGLLL
M4> LISLVENILVVVAIIKNRNLHSPMYYFICCLAVADMLVSVSNVVETLFMLLTEHGLLL

WT> VTAKMLQHLDNVIDIMICSSVVSSLSFLCTIAADRYITIFYALRYHSIMTTQRAVGIIL
M2> ATAGHRKNVAALR*----------
M3> VTAKMLQHLDNVIDIMICSSVVSSLSFLCTIAADRYITIFYALRYHSIMTTQRAVGIIL
M4> VTAKMLQHLDNVIDIMICSSVVSSLSFLCTIAADRYITIFYALRYHSIMTTQRAVGIIL

WT> VVWLASITSSSLFIVYHTDNAVIACLVTFFGVTLVFTAVLYLHMFILAHVHSRRITAL
M2> ----------
M3> VVWLASITSSSLFIVYHTDNAVIACLVTFFGVTLVFTAVLYLHVHLGPCPLKTHHGS
M4> VVWLASITSSSLFIVYHTDNAVIACLVTFFGVTLVFTAVLYLHLLIKICSSWPMSTQD

WT> HKSRRQTTSMKGAITLTILLGVFILCWGPFFLHLILILTCPTNPYCKCYFSHFNLFLI
M2> ----------
M3> P*----------
M4> ASRLSIRAVGRPLA*----------

WT> WTLIICNSLIDPLIYAYRSQELRKTLKELIFCSWCFAV*
M2> ----------
M3> ----------
M4> ----------

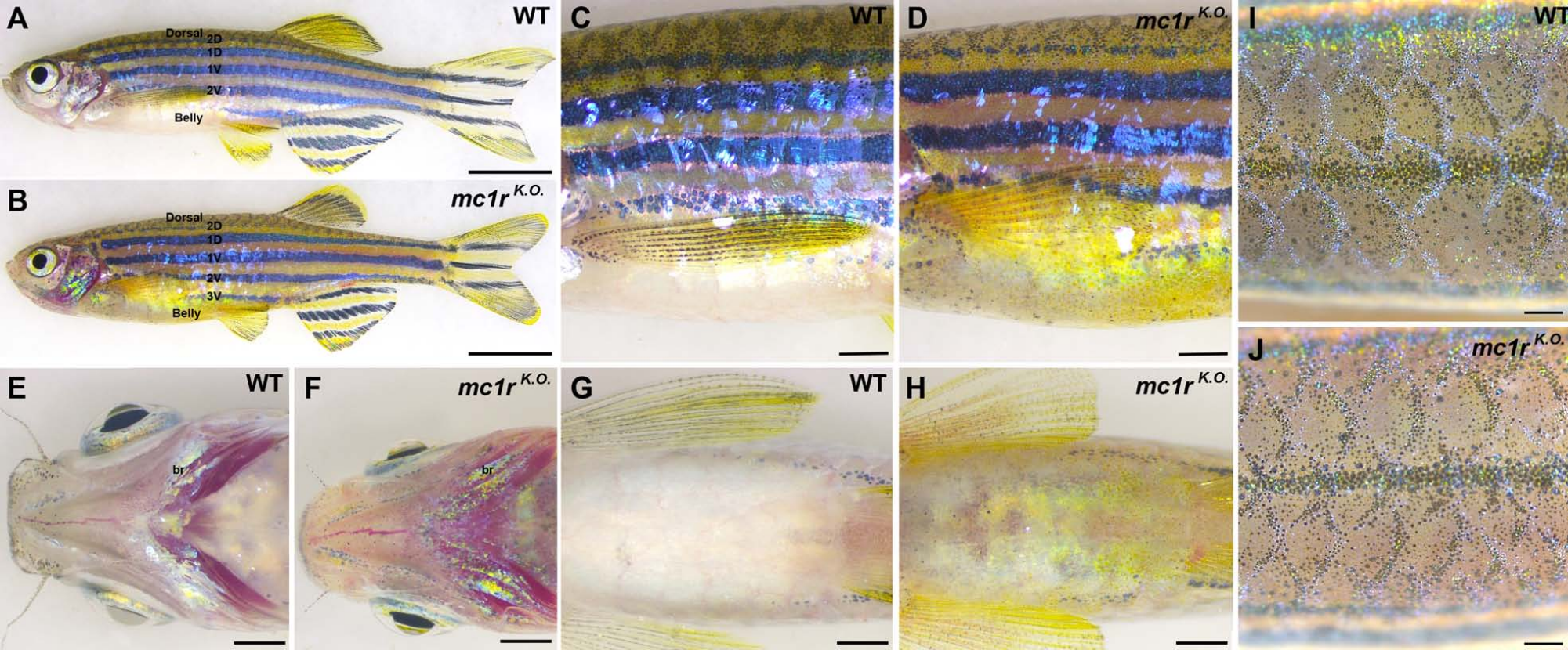
A
WT
Dorsal
2D
1D
1V
2V
Belly
B
mc1r K.O.
Dorsal
2D
1D
1V
2V
3V
Belly
C
WT
D
mc1r K.O.
I
WT
J
mc1r K.O.
E
WT
br
F
mc1r K.O.
br
G
WT
H
mc1r K.O.

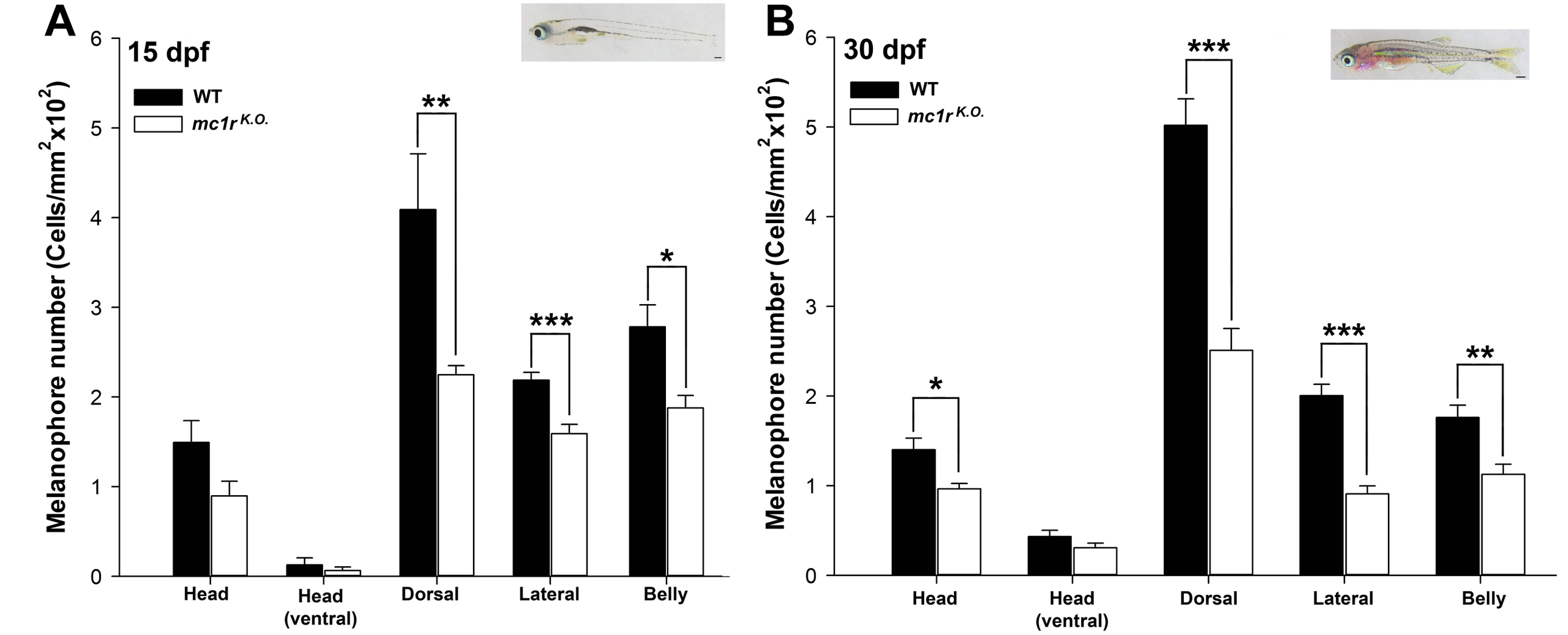
A
15 dpf
WT
mc1r K.O.
Melanophore number (Cells/mm2x102)
0
1
2
3
4
5
6
**
***
*
Head
Head (ventral)
Dorsal
Lateral
Belly
B
30 dpf
WT
mc1r K.O.
Melanophore number (Cells/mm2x102)
0
1
2
3
4
5
6
*
***
***
**
Head
Head (ventral)
Dorsal
Lateral
Belly

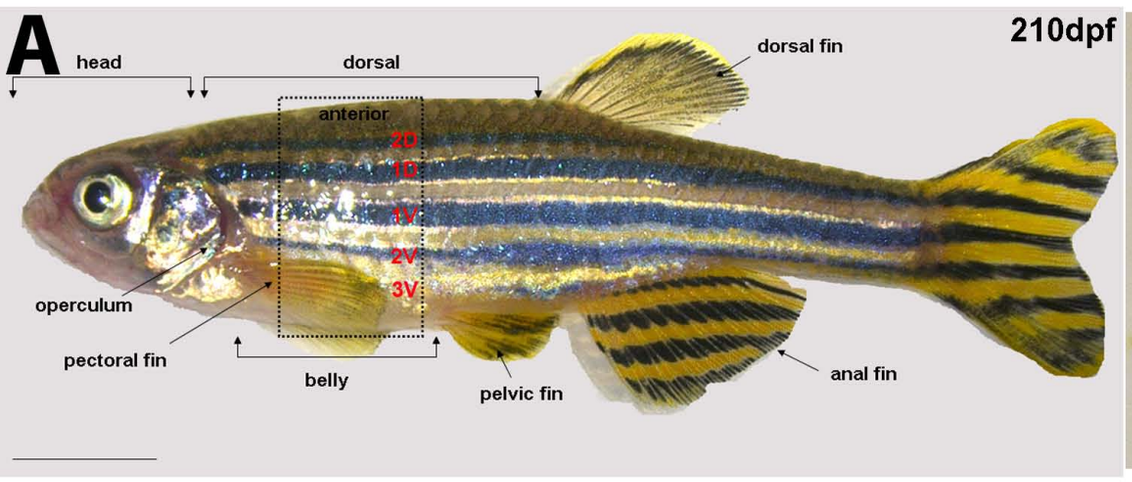
A
210dpf
head
dorsal
dorsal fin
anterior
2D
1D
1V
2V
3V
operculum
pectoral fin
belly
pelvic fin
anal fin

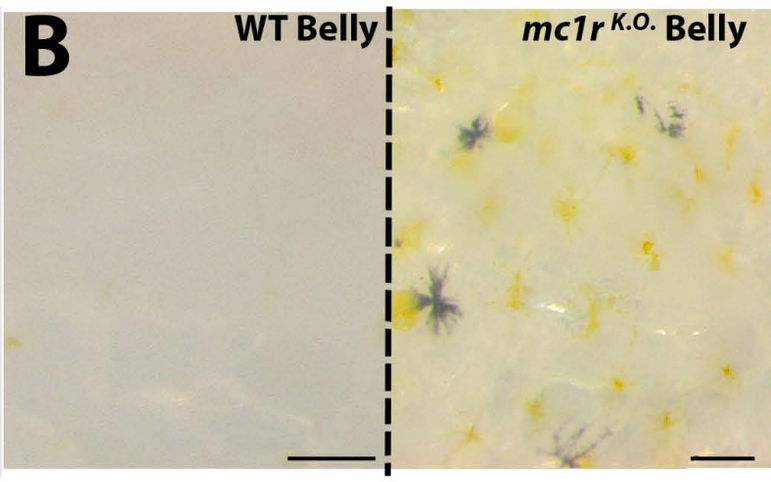
B
WT Belly
mc1r K.O. Belly

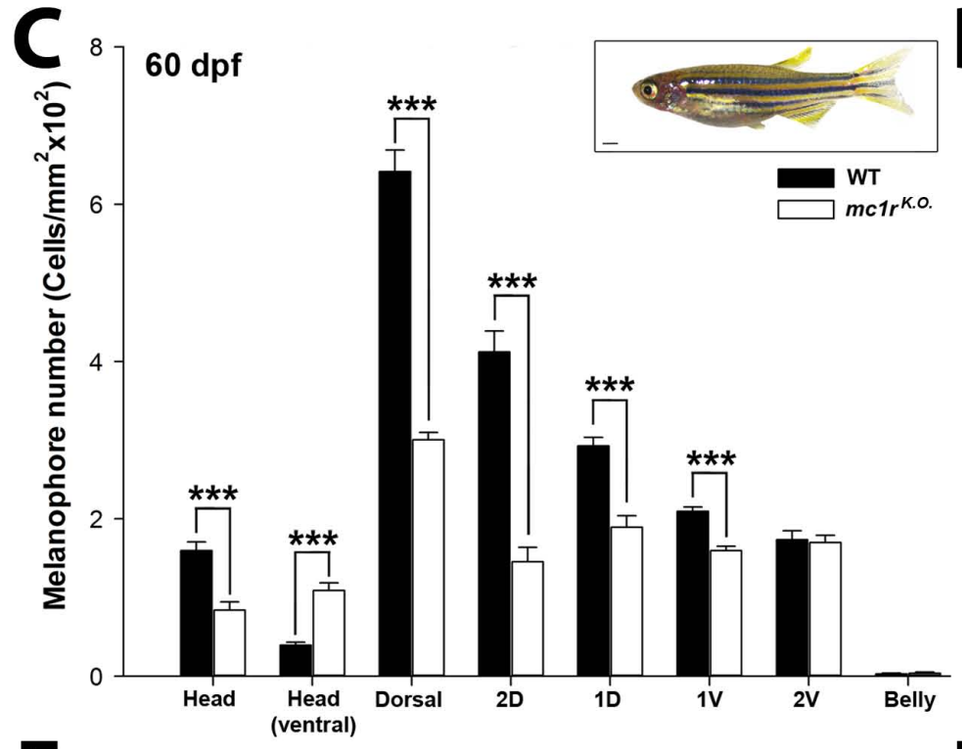
C
60 dpf
Melanophore number (Cells/mm2x102)
WT
mc1r K.O.
***
Head
Head (ventral)
Dorsal
2D
1D
1V
2V
Belly

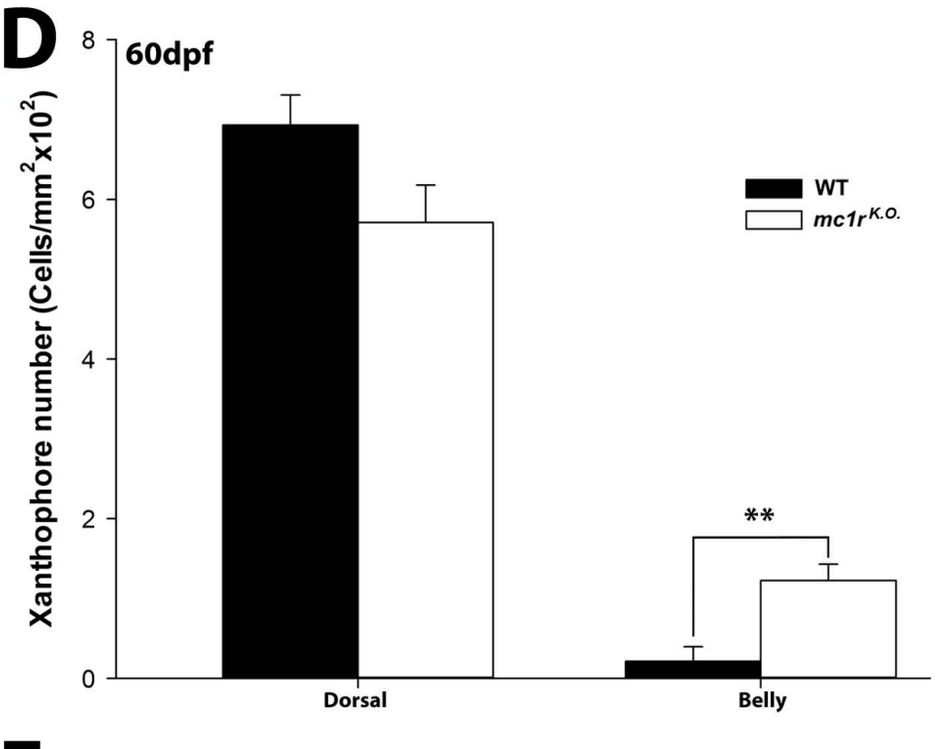
D
60dpf
Xanthophore number (Cells/mm2x102)
WT
mc1r K.O.
**
Dorsal
Belly

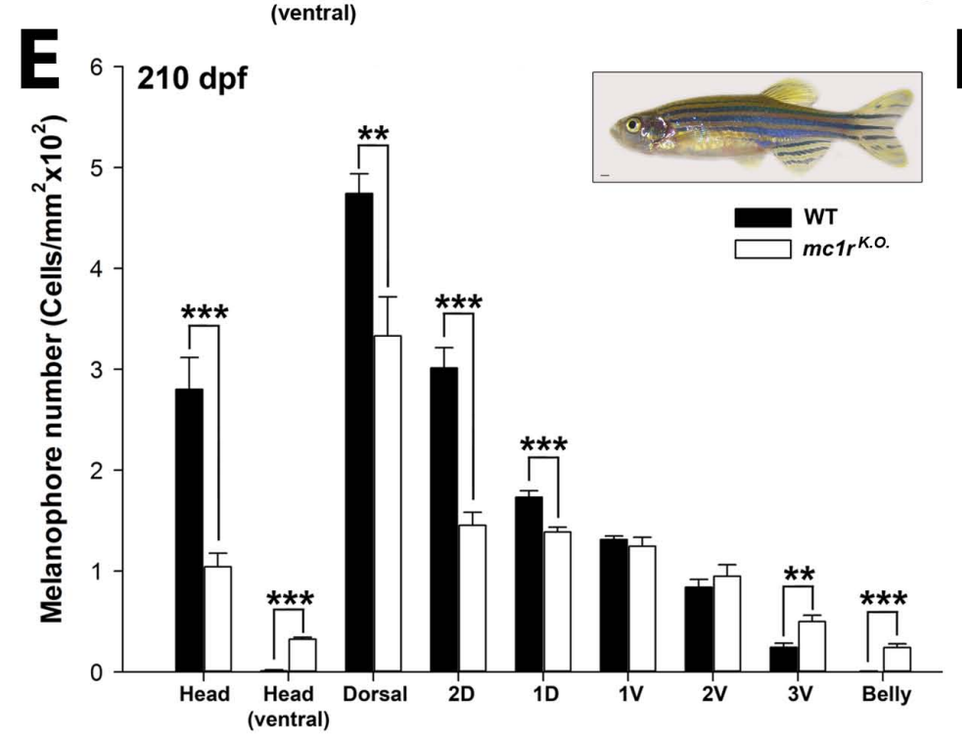
E
210 dpf
Melanophore number (Cells/mm2x102)
WT
mc1r K.O.
***
**
Head
Head (ventral)
Dorsal
2D
1D
1V
2V
3V
Belly

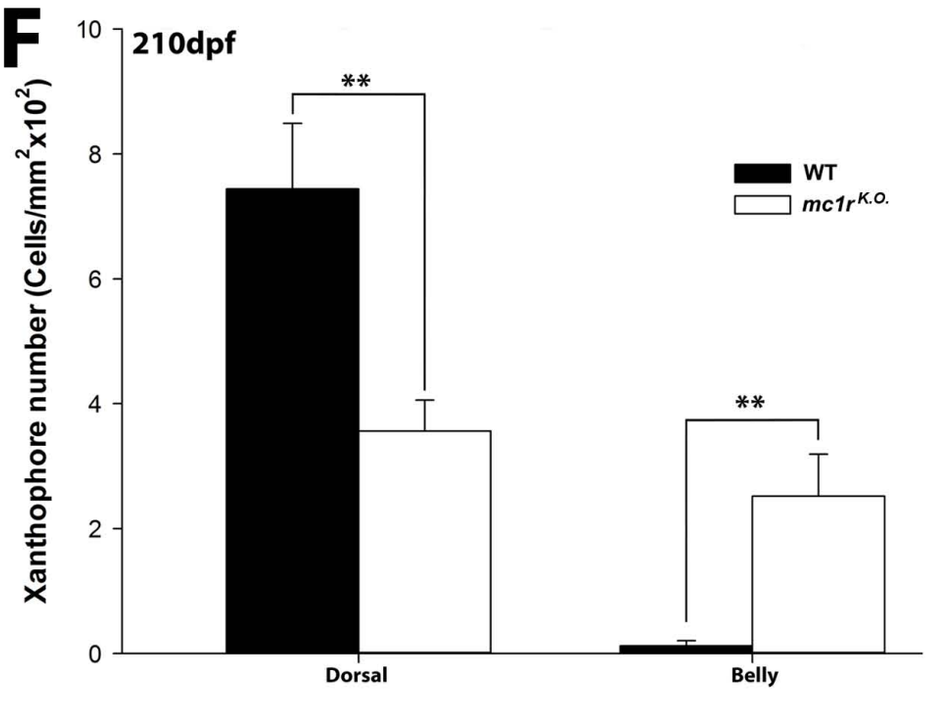
F
210dpf
Xanthophore number (Cells/mm2x102)
WT
mc1r K.O.
**
Dorsal
Belly

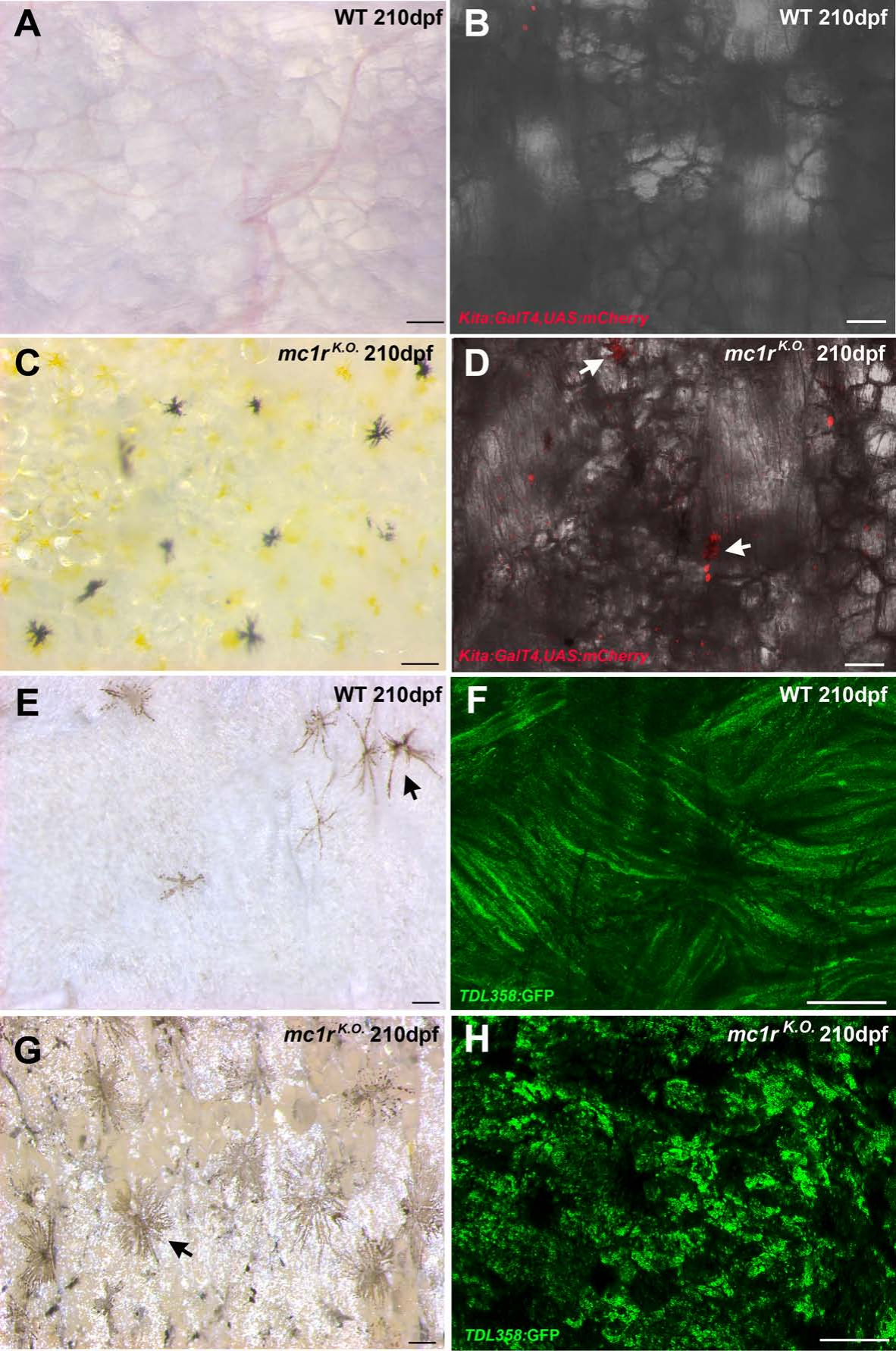
A
WT 210dpf
B
WT 210dpf
Kita:GalT4,UAS:mCherry
C
mc1r K.O. 210dpf
D
mc1r K.O. 210dpf
Kita:GalT4,UAS:mCherry
E
WT 210dpf
F
WT 210dpf
TDL358:GFP
G
mc1r K.O. 210dpf
H
mc1r K.O. 210dpf
TDL358:GFP

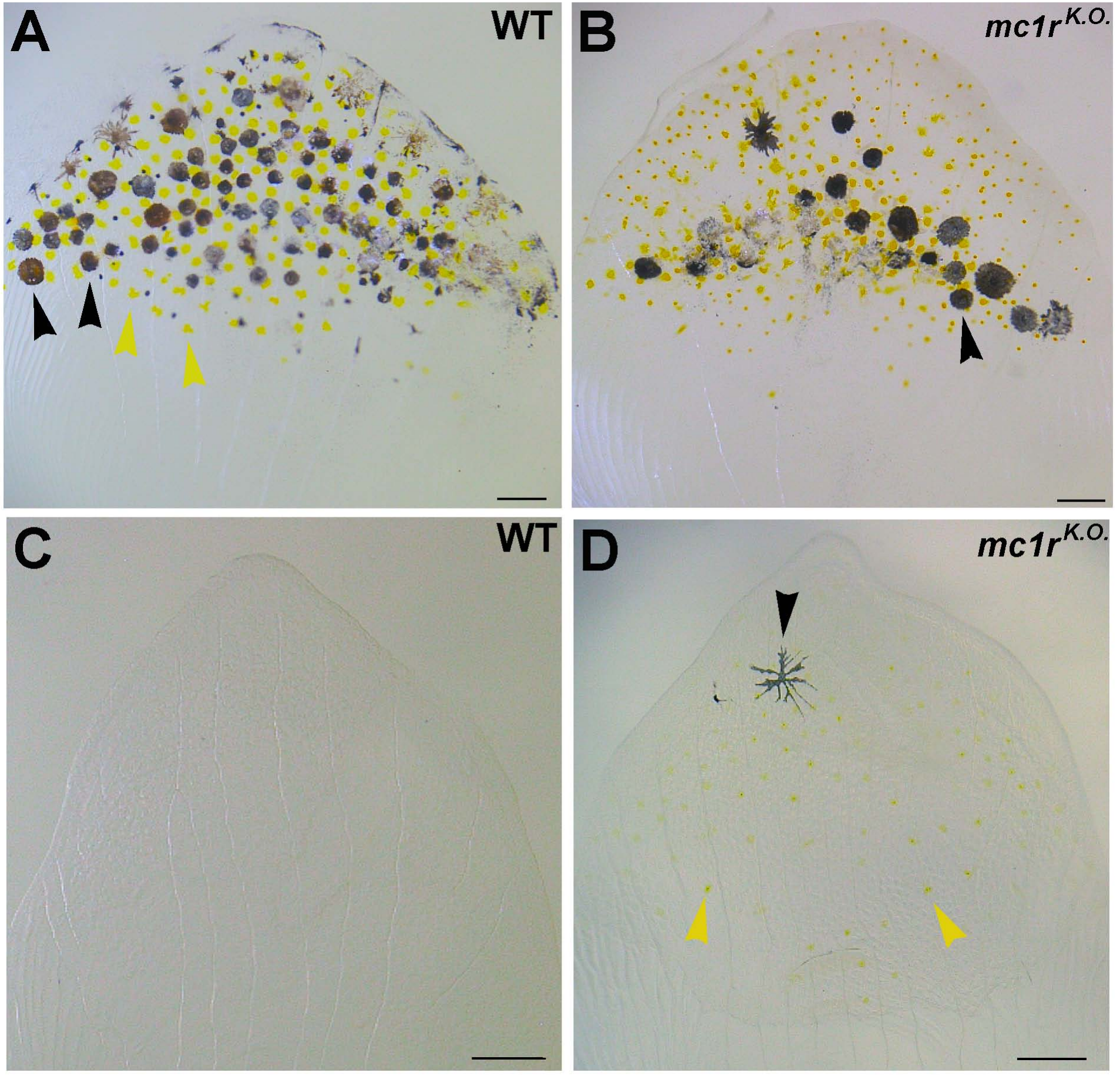
A
WT
B
mc1r K.O.
C
WT
D
mc1r K.O.

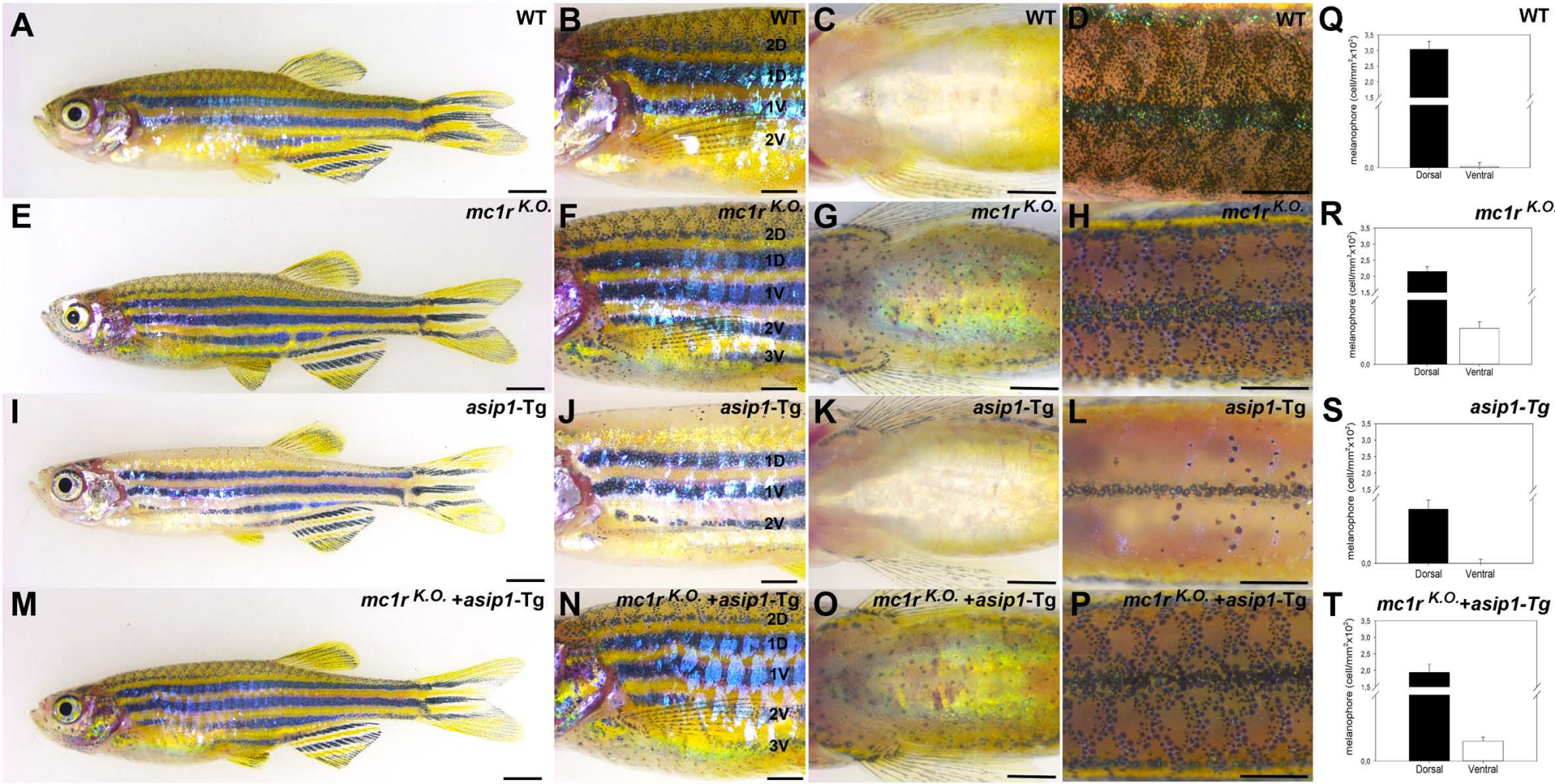
A
WT
B
WT
2D
1D
1V
2V
C
WT
D
WT
Q
WT
melanophore (cell/mm²x10²)
3,5
3,0
2,5
2,0
1,5
0,0
Dorsal
Ventral
E
mc1r K.O.
F
mc1r K.O.
2D
1D
1V
2V
3V
G
mc1r K.O.
H
mc1r K.O.
R
mc1r K.O.
I
asip1-Tg
J
asip1-Tg
1D
1V
2V
K
asip1-Tg
L
asip1-Tg
S
asip1-Tg
M
mc1r K.O. +asip1-Tg
N
mc1r K.O. +asip1-Tg
2D
1D
1V
2V
3V
O
mc1r K.O. +asip1-Tg
P
mc1r K.O. +asip1-Tg
T
mc1r K.O. +asip1-Tg

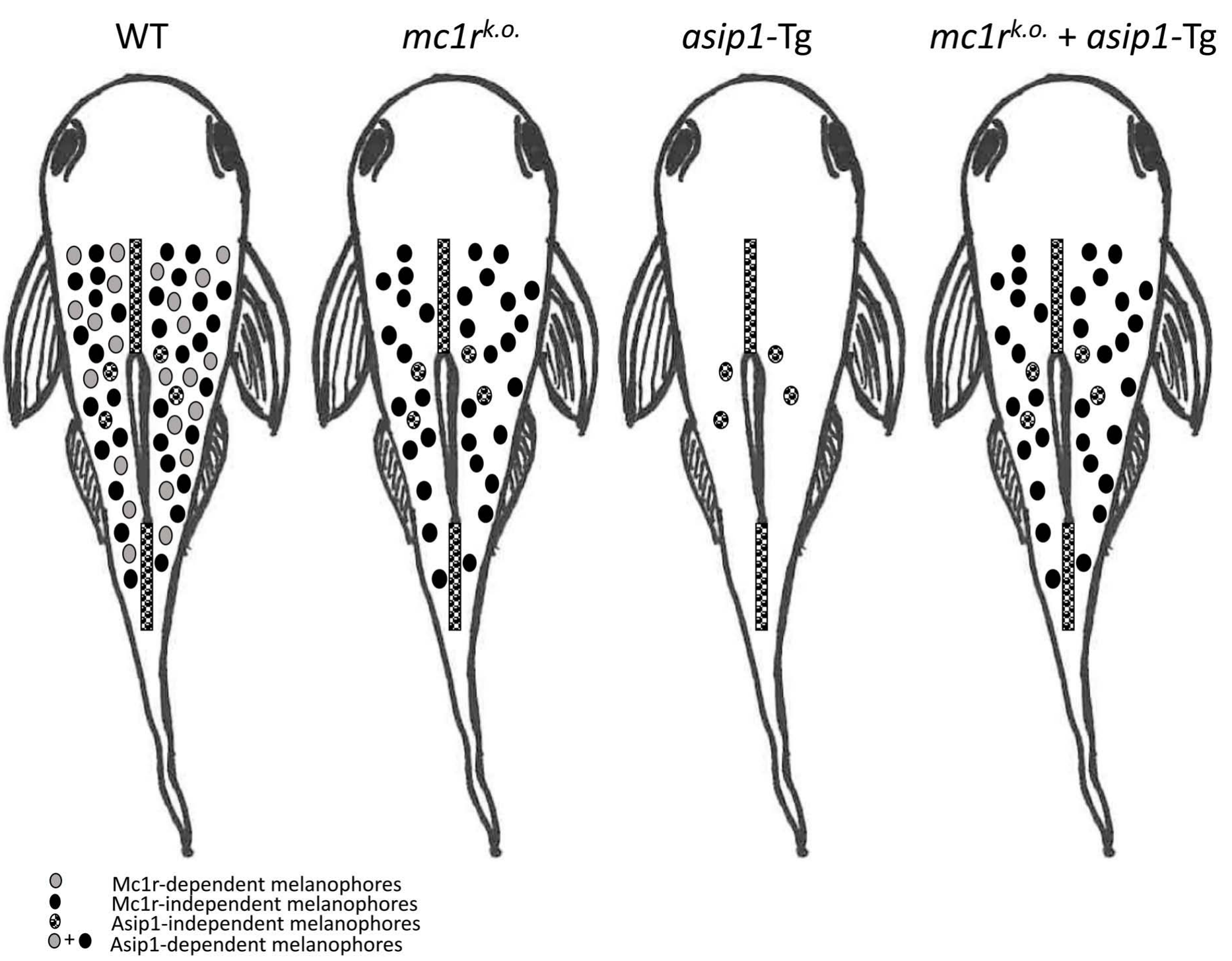
WT
mc1r k.o.
asip1-Tg
mc1r k.o. + asip1-Tg
Mc1r-dependent melanophores
Mc1r-independent melanophores
Asip1-independent melanophores
Asip1-dependent melanophores

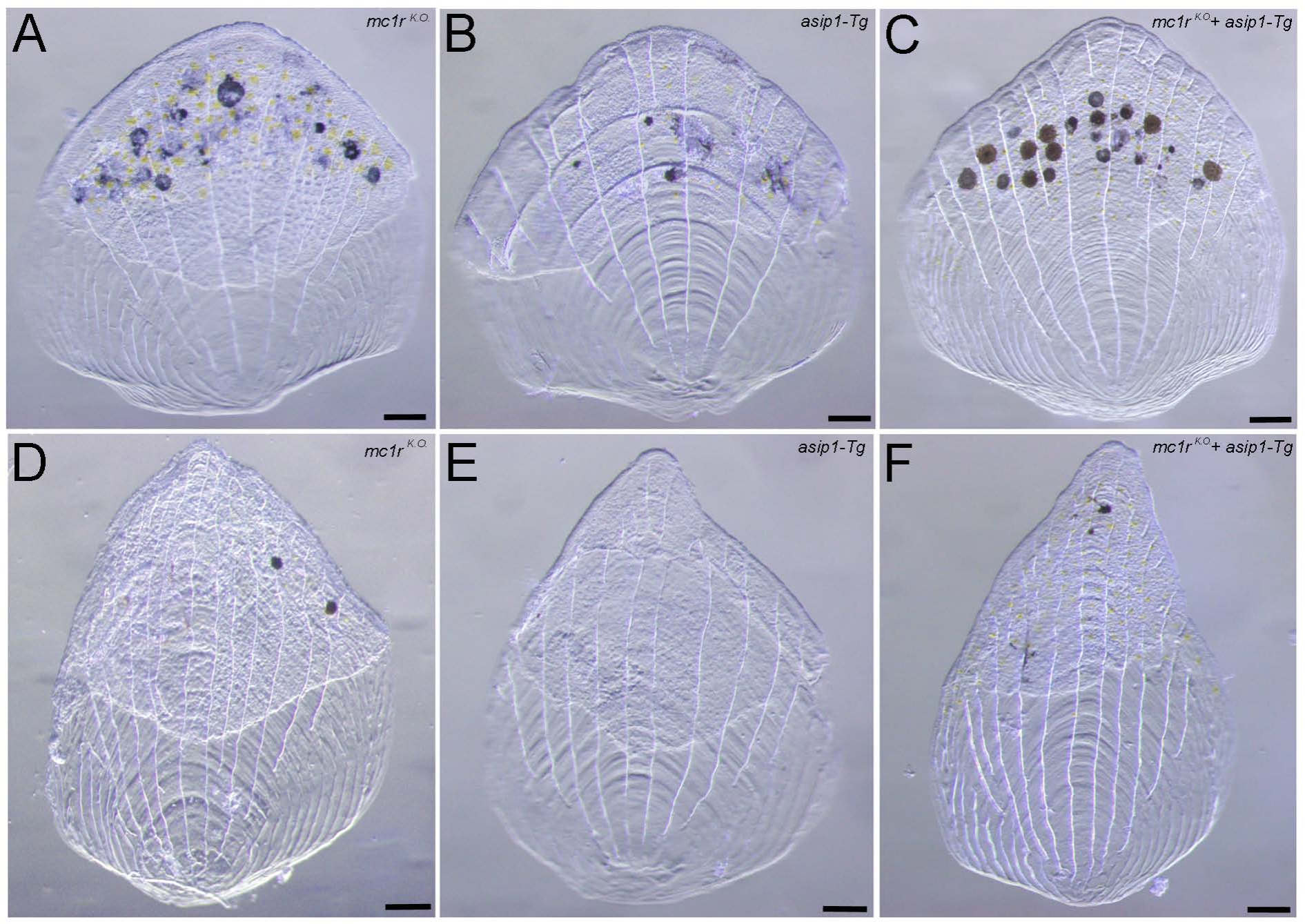
A
mc1r K.O.
B
asip1-Tg
C
mc1r K.O.+ asip1-Tg
D
mc1r K.O.
E
asip1-Tg
F
mc1r K.O.+ asip1-Tg